Description of the critical point symmetry in ^{124}Te by IBM-2*

Da-Li Zhang(张大立)[1)] Cheng-Fu Mu(穆成富)[2)]

Department of Physics, Huzhou University, Huzhou 313000, Zhejiang, China

Abstract: Based on the neutron and proton degrees of freedom, low-lying energy levels, $E2$, $M1$, and $E0$ transition strengths of nucleus ^{124}Te have been calculated by the neutron-proton interacting boson model. The calculated results are reasonably consistent with the experimental data. By comparing the key observables of the states at the critical point of $U_{\pi\nu}(5)$-$O_{\pi\nu}(6)$ transition with the experimental data and calculated results, we show that the ^{124}Te is a possible nucleus at the critical point of the second-order phase transition from vibration to unstable rotation, and such a critical point exhibits slight triaxial rotation. The 0_2^+ state of ^{124}Te can be interpreted as the lowest state of the first-excited family of the intrinsic levels in the critical point symmetry.

Keywords: ^{124}Te, low-lying structure, the critical point, $U_{\pi\nu}(5)$-$O_{\pi\nu}(6)$ transition

PACS: 21.10.Re, 21.60.Fw, 27.60.+j **DOI:** 10.1088/1674-1137/43/2/024104

1 Introduction

The characterization of the underlying structure of ^{124}Te is difficult, and it has attracted a significant amount of attention in various theoretical and experimental studies [1-6]. The ^{124}Te lies outside the major shell $Z = 50$ with two protons, and its ratio $E(4_1^+/2_1^+) = 2.07$ is very close to the spherical vibrator value of 2.00. This indicates that the ^{124}Te is a vibrational or U(5) symmetric nucleus. However, the energy levels spread of the two-phonon multiplets do not suggest a vibrational character in ^{124}Te. Meanwhile, the energy level of the lowest excited 0^+ state suggests that the ^{124}Te exhibits more γ-unstable or O(6) behavior; however, the $E2$ decays of the 0_2^+ state do not support the γ-soft rotational nature.

On the contrary, shape coexistence in the Te isotopes is still elusive [4]. The appearance of strong $\rho(E0, 0_2^+ \to 0_1^+)$ transition is an important spectroscopic fingerprint that mostly supports the shape coexistence in nucleus [7]. For ^{124}Te, the experimental value of the electric monopole transition strength $\rho^2(E0, 0_2^+ \to 0_1^+) \times 10^3$ is 12 ± 3 [8]. This value is very similar to the corresponding transition in the Cd isotopes; the latter demonstrates firm evidence for the nature of shape coexistence, providing strong support for the deformed intruder structure of the first-excited 0^+ state in ^{124}Te isotopes. However, it does not provide conclusive proof for the shape coexistence in ^{124}Te yet [4]. Meanwhile, systematic research on the known experimental information suggests that ^{124}Te may be an example of the nucleus at the $E(5)$ critical point [9]. Recent investigations indicate that ^{124}Te exhibits $E(5)$-like structure [5, 10]. However, the low-lying structure of ^{124}Te has still not been understood (see, e.g., Refs. [3, 10, 11] and references therein).

The $E(5)$ and $X(5)$ symmetries originally developed by Iachello [12, 13] correspond to an exact solution of the Bohr Hamiltonian for γ-independent potentials and an approximate solution of the Bohr-Hamiltonian for $\gamma \approx 0°$, respectively. From the Bohr-Hamiltonian with γ frozen at $\gamma = 30°$, a four dimensional critical point symmetry model called $Z(4)$ was introduced [14]. Most recently, another four-dimensional critical point symmetry called $T(4)$ was obtained from the Bohr-Hamiltonian with the β-soft potential and for a fixed value of γ with $0° \leqslant \gamma \leqslant 30°$ [15].

In the nuclear system, the $E(5)$ symmetry can be used to describe a nucleus at the critical point of the second-order phase transition from a spherical vibrator to a γ-soft rotor. In the interacting boson model (IBM-1) [16], which does not distinguish between the proton boson and neutron boson, the $E(5)$ represents a nucleus that is located at the critical point of the shape phase transition between the U(5) and O(6) symmetries. Because the neutron and proton degrees of freedom are explicitly taken into consideration, the proton-neutron interacting boson model (IBM-2)[16] has a complex phase diagram [17, 18]. The critic-

Received 27 October 2018, Published online 8 January 2019

* Supported by the National Natural Science Foundation of China (11475062, 11147148, 11747312)

1) E-mail: zdl@zjhu.edu.cn

2) E-mail: muchengfu@zjhu.edu.cn

al point of the second-order phase transition can occur at the phase transition from $U_{\pi\nu}(5)$ to $O_{\pi\nu}(6)$ symmetry and can be subsumed to the critical point of the second-order phase transition in IBM-1 [17-19]. Compared to their neighboring isotopes, nuclei at or close to the critical point of shape phase transition demonstrate drastic changes in the properties of the low-lying states, such as the energy levels, the $E2$ transition strengths, and $E2$ branching ratios [20]. However, so far, there has been no discussion on the critical point symmetry in the real nuclei for the phase transition between $U_{\pi\nu}(5)$ and $O_{\pi\nu}(6)$ in the IBM-2 phase diagram.

The low-lying levels of ^{124}Te have recently been examined with the (n,n',γ) reaction. The spins, level energies, $B(E2)$ transition probabilities, and multipole-mixing ratios were obtained [3]. The experiment provides the basis for an in-depth study of the low-lying structure of ^{124}Te. In this work, we study the low-lying structure of the ^{124}Te within the framework of the IBM-2, with a focus on the key observables of the critical point of the second-order transition between $U_{\pi\nu}(5)$ and $O_{\pi\nu}(6)$. We also calculate the low-lying energy levels and the $E2$, $M1$, and $E0$ transition strengths, and we compare the predictions of the critical point symmetry of the $U_{\pi\nu}(5)$-$O_{\pi\nu}(6)$ transition with the experimental data. We attempt to describe the critical point symmetry in the ^{124}Te, and reveal the low-lying structure of ^{124}Te in IBM-2 space.

The outline of the paper is as follows. In Section **2**, we introduce the Hamiltonians of IBM-2, $E2$, $M1$, and $E0$ operators, used in this work. The criteria adopted for the determination of the model parameters and the comparison of the numerical results with experimental data and the predictions of the critical point symmetry are presented in Section **3**. Finally, the conclusions and summary are provided in Section **4**.

2 Theoretical framework

The IBM-2 is an algebraic model, in which valence nucleons are coupled to form s_ρ bosons (angular momentum L=0) and d_ρ bosons (angular momentum $L=2$), where $\rho=\pi$ denotes proton bosons and $\rho=\nu$ denotes neutron bosons, respectively. The microscopic structure of the model suggests that there are only two significant terms: the pairing interaction between identical nucleons and the quadrupole-quadrupole interaction between nonidentical nucleons. The simple standard IBM-2 Hamiltonian [16, 21] is written as

$$\hat{H}=\varepsilon_{d\pi}\hat{n}_{d\pi}+\varepsilon_{d\nu}\hat{n}_{d\nu}+\kappa_{\pi\nu}\hat{Q}_\pi\cdot\hat{Q}_\nu, \quad (1)$$

where $\hat{n}_{d\rho}=d_\rho^\dagger\cdot\tilde{d}_\rho$ and $\hat{Q}_\rho=\left(s_\rho^\dagger\tilde{d}_\rho+d_\rho^\dagger s_\rho\right)^{(2)}+\chi_\rho\left(d_\rho^\dagger\tilde{d}_\rho\right)^{(2)}$ represent d-boson number operator and quadrupole operator, respectively. The parameter χ_ρ determines the type of the deformation of the quadrupole operator. $\varepsilon_{d\rho}$ is the energy of the d bosons relative to the s bosons, and $\kappa_{\pi\nu}$ is the strength of the quadrupole-quadrupole interaction between the neutron boson and the proton boson.

The Hamiltonian of Eq. (1) has a much richer shape phase structure, which contains $U_{\pi\nu}(5)$, $O_{\pi\nu}(6)$, $SU_{\pi\nu}(3)$, $\overline{SU_{\pi\nu}(3)}$, and $SU^*_{\pi\nu}(3)$ dynamical symmetries, corresponding to the spherical vibrator, γ-unstable rotor, axially symmetric prolate rotor, axially symmetric oblate rotor, and triaxial rotor, respectively. The shape phase transitions in nuclei can be characterized as the quantum phase transitions between the different dynamical symmetries in the IBM [17, 18, 22]. Although the standard IBM-2 Hamiltonian can provide a clearer space of dynamical symmetry, other physical dominant interactions must be included to describe the real nuclei more accurately. We use the following IBM-2 Hamiltonian in this study [16, 23, 24],

$$\hat{H}=\varepsilon_{d\pi}\hat{n}_{d\pi}+\varepsilon_{d\nu}\hat{n}_{d\nu}+\kappa_{\pi\nu}\hat{Q}_\pi\cdot\hat{Q}_\nu+\omega_{\pi\nu}\hat{L}_\pi\cdot\hat{L}_\nu+\hat{M}_{\pi\nu}, \quad (2)$$

where $\hat{L}_\rho=\sqrt{10}[d_\rho^\dagger\cdot\tilde{d}_\rho]^{(1)}$ is the angular momentum operator with a dipole proton-neutron interaction parameter $\omega_{\pi\nu}$, and $\hat{M}_{\pi\nu}=\lambda_2\left(s_\pi^\dagger d_\nu^\dagger-s_\nu^\dagger d_\pi^\dagger\right)^{(2)}\cdot\left(s_\pi\tilde{d}_\nu-s_\nu\tilde{d}_\pi\right)^{(2)}+\sum_{k=1,3}\lambda_k\left(d_\pi^\dagger d_\nu^\dagger\right)^{(k)}\cdot\left(\tilde{d}_\pi\tilde{d}_\nu\right)^{(k)}$ is the Majorana interaction; the Majorana parameters λ_k (k = 1, 2, 3) represent the strength of the Majorana interaction. If the Majorana term is not included in Eq. (2), the adopted parameters in the remaining four terms of Eq. (2) indicate that the nucleus described by the IBM-2 may be located on the the plane of $U_{\pi\nu}(5)$-$O_{\pi\nu}(6)$-$SU^*_{\pi\nu}(3)$, because the $\hat{L}_\pi\cdot\hat{L}_\nu$ only generates the physical rotational group $SO_{\pi\nu}(3)$ of the IBM-2 [16-18]. On the contrary, in Ref. [25] the authors proposed a new algebraic model $F(5)$ based on the Euclidean dynamical symmetry in five dimensions (Eu(5)), which can build a symmetry intermediate between the $E(5)$ and $X(5)$ symmetries [22]. However, the $F(5)$ cannot directly be defined in the IBM-1 or IBM-2 because of the noncompactness of the Eu(5) group [25].

The decay properties of the low-lying states, such as the $B(E2)$ transition probabilities, the magnetic dipole $B(M1)$ transition strengths and the $\rho^2(E0)$ values between the lowest 0^+ states are the characteristics of the phase structure. In the IBM-2, the $E2$ transition strength is given by the following expression

$$B(E2,J'\to J)=\frac{1}{2J'+1}|J\langle\left\|\hat{T}(E2)\right\|J'\rangle|^2, \quad (3)$$

where J' and J are the angular momenta for the initial and final states, respectively. The $\hat{T}(E2)=e_\pi\hat{Q}_\pi+e_\nu\hat{Q}_\nu$ is the $E2$ operator, where the operator Q_ρ is the same as in Eq. (1). The parameters e_π and e_ν are the effective charges of proton bosons and neutron bosons, respectively. The values of e_ν and e_π could be taken differently.

In the proton-neutron interacting boson model, the

magnetic dipole $M1$ transition operator is defined as

$$\hat{T}(M1)=\sqrt{\frac{3}{4\pi}}\left(g_\nu\hat{L}_\nu+g_\pi\hat{L}_\pi\right), \tag{4}$$

where the $\hat{L}_\rho$ is the same as in Eq. (2). The g_π and g_ν are the effective proton and neutron boson g-factors, respectively. Typically, one can take the values of $g_\pi=1$, $g_\nu=0$ in the calculations [21].

The $E0$ transition matrix element ρ in the IBM-2 is written as [26, 27]

$$\rho(E0,J'\to J)=\frac{Z}{eR^2}\left[\beta_{0\pi}\langle J\|\hat{T}_\pi(E0)\|J'\rangle +\beta_{0\nu}\langle\|\hat{T}_\nu(E0)\|JJ'\rangle\right] , \tag{5}$$

where $R=1.2A^{1/3}$fm, $\beta_{0\pi}$, and $\beta_{0\nu}$ are the effective monopole charges of proton and neutron boson in units of $e$fm^2, respectively. The $E0$ operator is expressed as $\hat{T}(E0)=\beta_{0\pi}\hat{T}_\pi(E0)+\beta_{0\nu}\hat{T}_\nu(E0)=\beta_{0\pi}\hat{n}_{d\pi}+\beta_{0\nu}\hat{n}_{d\nu}$, where the $\hat{n}_{d\rho}$ is the same as in Eq. (1).

3 Results and discussion

The ^{124}Te is located between the vibrational nucleus and the deformed nucleus [28]. The IBM provides a powerful tool to describe the nuclear shapes and the shape phase transitions. Several studies have used this approach to describe the properties of the low-lying states of ^{124}Te isotope. In IBM-1, early studies regarded the ^{124}Te as an example of O(6) symmetry; however, the energy levels of yrast states of ^{124}Te differ from the O(6) limit [29]. Further systematic investigations found that ^{124}Te was close to the U(5) symmetry [30, 31]. Moreover, recent results of experiments and calculations indicate that ^{124}Te may possess the $E(5)$ features [3, 9, 5, 10]. In IBM-2, the calculations with and without the mixed configuration suggest that ^{124}Te is an O(6)-like nucleus, but the $B(E2)$ decay pattern is not consistent with this symmetry [32]. A subsequent study showed that neither O(6) nor U(5) symmetries can describe the ^{124}Te well [33], although the potential energy surface of ^{124}Te exhibits an obvious manifestation of O(6) limit [34]. Another recent experiment and IBM calculation support that ^{124}Te demonstrates soft triaxial behavior [6]. Although the low-lying structure of the ^{124}Te is still not understood, it is indubitable that these results indicate that ^{124}Te is a transitional nucleus between vibration U(5) symmetry and γ-unstable O(6) symmetry in IBM, and might accompany with a slight soft triaxial rotation.

To describe the low-lying structure of ^{124}Te, we selected the doubly closed shell $^{132}_{50}$Sn$_{82}$ as the inert core. There are $N_\pi=1$ particle-like bosons beyond the $Z=50$ major shell, and $N_\nu=5$ hole-like neutron bosons from the $N=82$ shell closure; the total number of bosons is $N_B=6$. Considering that the proton bosons are particle-like and the neutron bosons are hole-like based on different single particle orbitals in ^{124}Te, we choose different relative energies for d neutron and proton boson in this case, i.e., $\varepsilon_{d\pi}\neq\varepsilon_{d\nu}$, similar to Refs. [35-37]. To describe the different type of valence neutrons and protons exhibiting opposite intrinsic quadrupole deformation, and to obtain the γ-unstable O(6) symmetry, we adopt $\chi_\pi+\chi_\nu=0$. To introduce some characteristics of the soft triaxial rotation in ^{124}Te, the value of χ_π and χ_ν should not be zero. In principle, the parameter $\varepsilon_{d\rho}$ mainly leads to vibrational solutions, while $\kappa_{\pi\nu}$ drives the system into a deformed shape, and the description of the electromagnetic properties is very sensitive to the parameters χ_ρ. The dipole interaction $\hat{L}_\pi\cdot\hat{L}_\nu$ can improve the rotational spectrum and can adjust the position of the 4_1^+ relative to 2_2^+ state; however, it does not affect the wave vectors [38]. The Majoranan operator mainly contributes to the mixed symmetry states including the scissors mode. All the free parameters in our calculations were fixed to reproduce the experimental energies and electromagnetic transition strengths of ^{124}Te. By fitting to the energy levels of the experimental data, especially for the 2_1^+ state, we obtain the parameters of IBM-2 in this study as follows: $\varepsilon_{d\pi}=1.220$MeV, $\varepsilon_{d\nu}=0.710$MeV, $\kappa_{\pi\nu}=-0.140$MeV, $\chi_\pi=-\chi_\nu=-1.00$, $\omega_{\pi\nu}=-0.055$MeV, $\lambda_1=-0.700$MeV, $\lambda_2=0.220$MeV, and $\lambda_3=-0.100$MeV. The IBM-2 Hamiltonian will be numerically diagonalized by using the NPBOS code [39]. In Fig. 1, we compare the calculated level energies with the experimental results [3, 40]. The experimental level energies in Fig. 1 are separated into different bands based only on their order of appearance; only the low-spin positive parity states with uniquely assigned spin and parity are displayed in the figure.

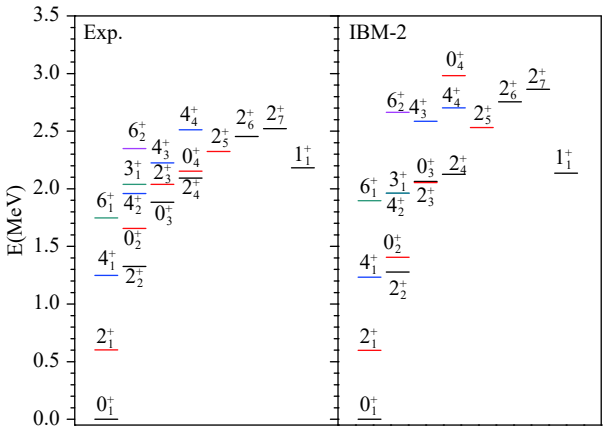

Fig. 1. (color online) Comparison of the calculated and experimental [3, 40] low-lying positive-parity levels of ^{124}Te.

Figure 1 shows that the theoretical levels are in good agreement with the corresponding experimental levels. In particular, the 6_1^+ state is dominated by two valence protons and is relatively unaffected by the increase of neut-

rons. The 6_1^+ states remain at a nearly constant excitation energy for even-even $^{122\text{-}130}$Te isotopes [3]. By introducing the dipole interaction term into the Hamiltonian [41-43], the structure of the yrast bands including the 6_1^+ level are reproduced by the theoretical predictions. Similar to the 6_1^+ state, the observed energy of 4_2^+ level is only changed by approximately 135 keV from ^{122}Te to ^{130}Te isotopes. The present calculation reproduces the experimental energy of the 4_2^+ level well. Meanwhile, the present calculated energies of the $2_{3,4,5}^+$, and 6_2^+ levels agree with the experimental observations. Even though the 0_2^+ level is clearly higher than that is expected for a two-phonon multiple state, the description of the first two excitation 0_+ states in energy sequence is satisfactory. Furthermore, the calculated energy level of the first scissor mode 1_1^+ perfectly reproduces the experimental data. However, there are some discrepancies between the experimental observations and the theoretical predictions for higher energy states, such as 2_6^+, and 2_7^+ states, which is a general feature of this model [44]. For the 0_4^+ state, the calculated level is significantly higher than the experimental level. The IBM-2 with the mixed configuration shows that 0_4^+ is an intruder state in ^{124}Te and is located outside the IBM-2 space [32].

In order to investigate the properties of the $E2$ transitions in ^{124}Te, the effective charges of the proton and neutron bosons were determined to reproduce the experimental $B(E2)$ values. Using the same method as in Refs. [45, 46] and exactly fitting to the experimental data of $B(E2, 2_1^+ \to 0_1^+) = 31(5)$ W.u., we obtain $e_\pi = 3.780$ $\sqrt{\text{W.u.}}$ and $e_\nu = 1.670$ $\sqrt{\text{W.u.}}$. The theoretical calculation of $B(E2)$ values for ^{124}Te in comparison with the available experimental data [1, 3, 10, 47-49] is given in Table 1.

Table 1 shows that the computed $B(E2)$ transition strengths are in overall agreement with the experimental data, although most cases of the experimental value have a large uncertainty. In particular, the typical strongly collective $E2$ transitions with tens of Weisskopf units are described by the theoretical predictions very well, some of them consist with each other within the experimental uncertainty. It is noteworthy that the experimental $B(E2, 4_1^+ \to 2_1^+)$ transition strength is 35.9(±17) W.u. in Ref. [3], which is taken from Ref. [6]. In Ref. [48], the experimental values show that the lower and upper limits of this transition probability are 27.3 and 163.5 W.u., respectively. Similar to Ref. [47], we adopt the experimental averaged value 54.51 W.u. for this transition; the details are provided in Ref. [50]. The experimental value agrees with the present calculated value. At the same time, the experimental relatively strong $B(E2)$ transitions, which are comparable with the experimental transition probability of the first-excited state 2_1^+ decay to the ground state with dozens of W.u., are reproduced by the calculated results perfectly except the $B(E2, 4_3^+ \to 2_2^+)$ transition strength. Furthermore, the calculated results are in good description of the properties of the experimental weakly collective $E2$ transitions with about one or even

Table 1. Experimental $E2$ transition strengths in ^{124}Te in units of W.u. are compared with the calculated results. The experimental data are taken from Refs. [1, 3, 10, 47-49]

$J_i^\pi \to J_f^\pi$	Expt.	IBM-2
$2_1^+ \to 0_1^+$	31_5^5	31.02
$4_1^+ \to 2_1^+$	54.51	48.06
$2_2^+ \to 2_1^+$	55.5_{99}^{109}	49.53
$2_2^+ \to 0_1^+$	0.83_{16}^{23}	0.24
$0_2^+ \to 2_1^+$	20_4^4	27.92
$0_3^+ \to 2_2^+$	50.00	48.51
$4_2^+ \to 2_2^+$	14.1_{28}^{30}	29.94
$4_2^+ \to 4_1^+$	12.7_{59}^{74}	27.06
$4_2^+ \to 2_1^+$	4.3_9^9	0.31
$3_1^+ \to 2_2^+$	59_{10}^{10}	42.65
$2_3^+ \to 0_1^+$	0.26_4^4	2.08
$2_3^+ \to 2_1^+$	0.025_3^4	0.50
$2_3^+ \to 2_2^+$	$\leqslant 2.7_{15}^{19}$	4.03
$2_3^+ \to 4_1^+$	0.81_{81}^{104}	5.38
$2_3^+ \to 3_1^+$	0.26_4^5	0.37
$2_4^+ \to 2_2^+$	0.29_{33}^{39}	1.85
$2_4^+ \to 2_1^+$	1.6_3^3	1.39
$2_4^+ \to 0_1^+$	0.053_{14}^{17}	2.16
$0_4^+ \to 2_1^+$	< 0.5	0.04
$0_4^+ \to 2_2^+$	< 50	0.03
$1_1^+ \to 2_1^+$	1.2_3^4	4.99
$1_1^+ \to 2_2^+$	0.74_{38}^{38}	1.13
$4_3^+ \to 2_2^+$	13.4_{39}^{49}	1.16
$4_3^+ \to 4_1^+$	6.7_{20}^{23}	2.89
$4_3^+ \to 2_1^+$	1.9_5^6	0.95
$2_5^+ \to 2_2^+$	0.61_{30}^{40}	1.02
$2_5^+ \to 2_1^+$	0.06_6^7	0.15
$2_5^+ \to 0_1^+$	0.078_{42}^{50}	0.09
$2_6^+ \to 2_2^+$	1.6_5^5	1.67
$2_6^+ \to 4_1^+$	1.7_4^5	0.00
$2_6^+ \to 2_1^+$	0.046_6^8	0.23
$2_6^+ \to 0_1^+$	0.12_2^3	0.01
$4_4^+ \to 4_1^+$	2.6_7^9	0.10
$4_4^+ \to 2_1^+$	0.051_{22}^{28}	0.72
$2_7^+ \to 2_1^+$	4.0_4^4	0.56
$2_7^+ \to 2_2^+$	0.20_{11}^{10}	0.00
$2_7^+ \to 4_1^+$	< 1.6	1.10

less than one W.u.. The theoretical $E2$ transition strengths from the scissor mode 1^+_1 to the 2^+_1 and 2^+_2states are in agreement with the corresponding experimental data, although the theoretical values are slightly higher than the experimental data test

To identify where the ^{124}Te can be placed in the $U_{\pi\nu}(5)$ to $O_{\pi\nu}(6)$ transition, we focus on a set of key observables [51], such as the energy ratios $R_{4_1/2_1}=E(4^+_1)/E(2^+_1)$, $R_{2_2/2_1}=E(2^+_2)/E(2^+_1)$, $R_{0_2/2_1}=E(0^+_2)/E(2^+_1)$, $R_{0_3/0_2}=E(0^+_3)/E(0^+_2)$, and the $B(E2)$ ratios $R_{B,42}=B(E2,4^+_1\to 2^+_1)/B(E2,2^+_1\to 0^+_1)$, $R_{B,22}=B(E2,2^+_2\to 2^+_1)/B(E2,2^+_1\to 0^+_1)$ and $R_{B,02}=B(E2,0^+_2\to 2^+_1)/B(E2,2^+_1\to 0^+_1)$, which reflect the characteristics of the nucleus behavior at critical point of the phase transition from $U_{\pi\nu}(5)$ to $O_{\pi\nu}(6)$ in IBM-2 space [17]. These observables are the most crucial nuclear structure indicators [52]. Some indicators can even distinguish the first-order quantum phase transition from the second-order quantum phase transition [53-55]. The values of these key observables at the critical point of the phase transition from $U_{\pi\nu}(5)$ to $O_{\pi\nu}(6)$ for infinite numbers of bosons [12], as well as the experimental data and the calculated results in ^{124}Te, are listed in Table 2 for comparison.

Table 2. Comparison of the key observables of the states at the critical point of the $U_{\pi\nu}(5)$-$O_{\pi\nu}(6)$ transition (taken from Ref. [12] and denoted as CPST), the experimental data of ^{124}Te (taken from Refs. [1, 3, 47-49] and labeled as ^{124}Te) and the calculated results (labeled as IBM-2).

	CPST	^{124}Te	IBM-2
$R_{4_1/2_1}$	2.20	2.07	2.06
$R_{2_2/2_1}$	2.20	2.20	2.13
$R_{0_2/2_1}$	3.03	2.75	2.35
$R_{0_3/0_2}$	1.18	1.14	1.46
$R_{B,42}$	1.68	1.74	1.55
$R_{B,22}$	1.68	1.79	1.60
$R_{B,02}$	0.86	0.65	0.90

Table 2 shows that the overall agreement is well. On the energy ratios, the experimental ratio $R_{2_2/2_1}$ is almost exactly reproduced to the critical point of the $U_{\pi\nu}(5)$-$O_{\pi\nu}(6)$ transition. The experimental ratio $R_{0_3/0_2}$ is very close to the value of CPST. Meanwhile, the experimental energy of the 0^+_2 state, relative to $E(2^+_1)$, satisfactorily matches the predicted value of CPST. The experimental $R_{4_1/2_1}$ lies between $U_{\pi\nu}(5)$ ($R_{2_2/2_1}=2.00$) and $O_{\pi\nu}(6)$ ($R_{2_2/2_1}=2.50$) limits, although it deviates slightly from the predicted one. On the $B(E2)$ ratios, the experimental $R_{B,42}$ is well reproduced by the theoretical prediction and clearly points to a structure intermediate between $U_{\pi\nu}(5)$ ($R_{B,42}=2.00$) and $O_{\pi\nu}(6)$($R_{B,42}=10/7$). Meanwhile, the experimental value of $R_{B,22}$ also approaches the predicted value of the critical point theory. In particular, the information of $R_{B,02}$ is a signature for identifying the $U_{\pi\nu}(5)$ from the $O_{\pi\nu}(6)$ symmetry. In $U_{\pi\nu}(5)$ limit, the $B(E2,0^+_2\to 2^+_1)$ transition strength is two times larger than $(B(E2,2^+_1\to 0^+_1)$. In $O_{\pi\nu}(6)$ limit, the $B(E2,0^+_2\to 2^+_1)$ transition is forbidden [56]. Here, both the experimental and theoretical values of the $R_{B,02}$ can correctly reflect the nature of the $B(E2,0^+_2\to 2^+_1)$ transition, although the calculated value overestimates the experimental value by approximately 1.5 times. Therefore, all the available experimental information on the key observables for ^{124}Te is in good agreement with the predictions of critical point of the $U_{\pi\nu}(5)$-$O_{\pi\nu}(6)$ transition. Meanwhile, Table 2 also shows that the present calculation of the characteristic feature of ^{124}Te is remarkable. However, the $R_{0_2/2_1}$ of CPST seems larger than the IBM's in Table 2; this is because the calculation of the CPST is given for the infinite−N_B limit [12, 51]. For a finite number of bosons, Ref. [17] showed that the $R_{0_2/2_1}$ of a nucleus at the critical point of the phase transition from $U_{\pi\nu}(5)$ to $O_{\pi\nu}(6)$ with $N_\pi=N_\nu=5$ is 2.48, which agrees the result of the present calculations. From the above discussion, we conclude that the ^{124}Te may be a nucleus at the critical point of the $U_{\pi\nu}(5)$-$O_{\pi\nu}(6)$ transition. Consequently, the 0^+_2 state is the lowest possible state of the first-excited family of intrinsic levels predicted by the critical point symmetry.

An advantage of IBM-2 over IBM-1 is that the former can study the influence of the critical point symmetry on magnetic dipole transitions between the low-lying states [23]. In IBM-2, the pure $O_{\pi\nu}(6)$ symmetry can be obtained only with $\chi_\pi=\chi_\nu=0$. In this case, there does not exist any asymmetry between χ_π and χ_ν. This implies that the mixed symmetry components could not mix into the low-lying states. Therefore, the $M1$ transitions between these states are forbidden in $O_{\pi\nu}(6)$ limit [21]. The theoretical predictions show that the $B(M1)$ transition strengths among the low-lying states almost vanish when a nucleus is at the critical point of the $U_{\pi\nu}(5)$-$O_{\pi\nu}(6)$ transition [17]. For the scissors mode state 1^+_1, the $B(M1,1^+_1\to 0^+_1)$ transition strength is $3N_\pi N_\nu(g_\nu-g_\pi)^2/4\pi(2N_B+1)$ for $O_{\pi\nu}(6)$ limit; however, it is forbidden for $U_{\pi\nu}(5)$ limit. The $B(M1,1^+_1\to 0^+_2)$ value is $3N_\pi N_\nu(g_\nu-g_\pi)^2/\pi N_B(N_B-1)$ for $U_{\pi\nu}(5)$ limit, whereas it vanishes for $O_{\pi\nu}(6)$ limit [23, 57, 58]. At the critical point of $U_{\pi\nu}(5)$-$O_{\pi\nu}(6)$ transition, the 1^+_1 state allows $M1$ decays to first and second 0^+ states. In the case of ^{124}Te, the $B(M1,1^+_1\to 0^+_1)$ is $0.10\,\mu^2_N$ for $O_{\pi\nu}(6)$ limit, and $B(M1,1^+_1\to 0^+_2)$ is $0.50\,\mu^2_N$ for $U_{\pi\nu}(5)$ limit, with the typical values $g_\pi=$ land $g_\nu=0$. Indeed, only a few $M1$ transitions, with very small absolute values of $B(M1)$, among the low-lying states in ^{124}Te have been measured [49, 59]. By using Eq. (4) and also taking $g_\pi=1$ and $g_\nu=0$, the calculated $M1$ transition probabilities, as well as the corresponding available experimental data for the scissors mode and the low-lying states in ^{124}Te, are provided in Table 3.

Table 3. Comparison of the calculated $M1$ transition strengths (in units of μ_N^2) and the experimental data for ^{124}Te. The experimental data are taken from Refs. [11, 48, 49, 60].

Transition	Expt.	IBM-2
$2_2^+ \to 2_1^+$	0.0003	0.006
$2_3^+ \to 2_2^+$	0.004	0.025
$2_3^+ \to 2_1^+$	0.013	0.072
$2_4^+ \to 2_2^+$	0.001	0.031
$2_4^+ \to 2_1^+$	0.004	0.075
$1_1^+ \to 0_1^+$	0.04	0.029
$1_1^+ \to 0_2^+$		0.034

From Table 3, it can be seen that all the experimental $B(M1)$ transition strengths between the lowest 2_+ states are of the order of approximately 0.01 μ_N^2 or even less, which is far from the typical $B(M1)$ value of the mixed symmetry state. This demonstrates that the observed $M1$ transitions are in qualitative agreement with the predictions of the critical point symmetry of the $U_{\pi\nu}(5)$-$O_{\pi\nu}(6)$ transition. At the same time, Table 3 shows that the calculated results reasonably reproduce the characteristics of the $M1$ transitions among low-lying states. In particular, the calculated $B(M1, 1_1^+ \to 0_1^+)$ strength is close to the experimental one, which is comparable to the predicted value of the critical point between the $U_{\pi\nu}(5)$ and $O_{\pi\nu}(6)$ limits. This indicates that both the experimental and the calculated results of the $B(M1, 1_1^+ \to 0_1^+)$ transition reflect the property of the nucleus at the critical point of the $U_{\pi\nu}(5)$-$O_{\pi\nu}(6)$ transition. Unfortunately, the $B(M1, 1_1^+ \to 0_2^+)$ strength in ^{124}Te has not been measured, the calculated value for this transition is 0.035 μ_N^2, locating between the $U_{\pi\nu}(5)$ and $O_{\pi\nu}(6)$ transition similar to the case of $B(M1, 1_1^+ \to 0_1^+)$ transition. All these results indicate that both the calculated and experimental $M1$ transitions are consistent with the characteristic behavior of the ^{124}Te nucleus at the critical point of the $U_{\pi\nu}(5)$-$O_{\pi\nu}(6)$ transition.

However, some deviations between the theoretical and experimental $M1$ transition strengths are also are displayed in Table 3; all the calculated $M1$ values are slightly larger than the corresponding experimental values. In IBM-2, $\chi_\pi = -\chi_\nu \neq 0$ leads to a spectrum with many O(6) features. In addition, some mixed symmetry components from the asymmetry of χ_π and χ_ν mix into the low-lying states beside the pure mixed symmetry states at higher energies [21, 61]. On the contrary, $\chi_\pi = -\chi_\nu \neq 0$ makes the nucleus have some features of the $SU^*_{\pi\nu}(3)$ symmetry, because the proton and neutron have opposite types of deformation [18]. The calculated $B(M1)$ values among the lowest states are systematically slightly larger than the experimental data, which implies that the description of ^{124}Te with the characteristics of the $SU^*_{\pi\nu}(3)$ is slightly rather than the actual nucleus. Furthermore, the small $B(M1)$ values among the low-lying states in ^{124}Te also indicate that ^{124}Te may contain some components of $SU^*_{\pi\nu}(3)$ symmetry. Therefore, the ^{124}Te may be the nucleus at the critical point of the $U_{\pi\nu}(5)$-$O_{\pi\nu}(6)$ transition and with a slight $SU^*_{\pi\nu}(3)$ symmetry.

The electric monopole transition strengths between 0^+ states can be considered as a characteristic of shape coexistence [7] and quantum phase transitions [62], and it can reflect the properties of $E(5)$ dynamical symmetry [9]. In fact, the $\rho^2(E0, 0_2^+ \to 0_1^+)$ value of ^{124}Te has been measured [8]. However, the $\rho^2(E0)$ value on the first-excited 0^+ state in ^{124}Te has not been understood yet, as mentioned in the introduction [4]. In IBM, the $E0$ transitions do not occur in the U(5) dynamical limit, because $E0$ operator is proportional to $\hat{n}_d$ [63].While in O(6) limit, the selection rules require the $E0$ transition from the 0_2^+ to ground state to be forbidden [64]. For the predicted $E(5)$ symmetry, the 0_2^+ level, which is the lowest member (zero phonon) of the first-excited family, should have an allowed $E0$ branch to the 0_1^+ state. However, so far, the studies of the behavior of $E(5)$ symmetry in ^{124}Te have not provided a detailed analysis of the properties of $E0$ transitions. In IBM-2 space, all the symmetrical states have correspondence with the IBM-1 states; therefore, IBM-2 subsumes the critical point of second-order transition of IBM-1[17, 23]. The critical point symmetry of $U_{\pi\nu}(5)$-$O_{\pi\nu}(6)$ has considerably similarity to the predictions of the $E(5)$ symmetry [17]. Subsequently, the 0_2^+ level should also have an allowed $E0$ decay to the ground state in this prediction of the critical point symmetry. We take the values of parameters $\beta_{0\nu}$ and $\beta_{0\pi}$ as in Ref. [65], namely, $\beta_{0\nu} = 0.25$ and $\beta_{0\pi} = 0.10$ $e\text{fm}^2$. The calculated $\rho^2(E0, 0_2^+ \to 0_1^+) \times 10^3$ value is 11.00, which is consistent with the experimental data within the experimental uncertainty. The theoretical and experimental $E0$ transitions prove that the 0_2^+ state may be interpreted as the lowest state of the first-excited family of intrinsic levels in the critical point symmetry of second order $U_{\pi\nu}(5)$-$O_{\pi\nu}(6)$ transition.

It is well known that the low-lying yrast states in other Te isotopes such as $^{112, 114}$Te show similar behavior, i.e., typical vibrational like spectra, but other properties deviate from the vibrator's [6, 66-68]. These Te isotopes are located around the midshell ^{118}Te. The large-scale shell-model calculations indicate that the behavior of the $B(E2)$ values of these nuclei is related to the competition between the seniority coupling and the neutron-proton correlations. From the viewpoint of the IBM model, ^{112}Te is below the midshell ^{118}Te; it has $N_\nu = 5$ bosons beyond $N = 50$ major shell. Both ^{112}Te and ^{124}Te have the same numbers of bosons with $N_\pi = 1$ and $N_\nu = 5$; therefore, they show similar properties of spectrum. As for ^{114}Te, the measured ratio of $B(E2, 4_1^+ \to 2_1^+)$ to $B(E2, 2_1^+ \to 0_1^+)$ is less than one, which is a very unusual deformation; no theor-

etical models can provide a satisfactory description [68].

4 Conclusion

In summary, the low-lying structure of the ^{124}Te was investigated within the framework of IBM-2. The calculated low-lying energy levels are in good agreement with the corresponding experimental data. In particular, the 6_1^+, 4_2^+ levels, which are maintain a nearly constant excitation energy from ^{122}Te to ^{130}Te isotopes, have been satisfactorily reproduced by using the calculated results. In addition, the first two excited 0^+ states were described well in the energy sequence, although the 0_2^+ level is clearly higher than that is expected for a two-phonon multiple state. Furthermore, the calculated energy level of the first scissor mode 1_1^+ perfectly reproduces the experimental data.

The calculations show that the computed $B(E2)$ transition strengths are in the overall agreement with the experimental data. The observed typical strongly collective $E2$ transitions with tens of Weisskopf units, and most of the experimental relatively strong $B(E2)$ transitions comparable to the experimental $B(E2,2_1^+\rightarrow 0_1^+)$ transition probability with dozens of W.u., are reproduced by the theoretical predictions nicely. Furthermore, the calculated results provide accurate description of the properties of the experimentally weakly collective $E2$ transition with approximately one or even less than one W.u.. Particularly, the theoretical $E2$ transitions from the scissor mode 1_1^+ to the 2_1^+ and 2_2^+ states are in good agreement with the corresponding experimental data, although the theoretical values are slightly higher than the experimental data.

By comparing the key observables of the states at the critical point of the $U_{\pi\nu}(5)$-$O_{\pi\nu}(6)$ transition with the experimental data and the IBM-2 calculations, we show that both the experimental data and the theoretical results of the ^{124}Te agree with the predicted properties of the states at the critical point of the phase transition from $U_{\pi\nu}(5)$ to $O_{\pi\nu}(6)$ very well. This indicates that the ^{124}Te may be a nucleus at the critical point of the $U_{\pi\nu}(5)$-$O_{\pi\nu}(6)$ transition. Consequently, the 0_2^+ state is the lowest possible state of the first-excited family of the intrinsic levels predicted by the critical point symmetry.

At the same time, the characteristics of the $B(M1)$ transition strengths among the low-lying states are consistent with the predictions of the critical point of the transition from $U_{\pi\nu}(5)$ to $O_{\pi\nu}(6)$, and there is good agreement between the experiment and the theory for characteristics of the $B(M1)$ transition strengths. Especially, both the experimental and theoretical $B(M1,1_1^+\rightarrow 0_1^+)$ values are located between the $U_{\pi\nu}(5)$ and $O_{\pi\nu}(6)$ limits. By analyzing the calculated results and the structure parameters of the quadrupole operators in this work, all quantities support that the ^{124}Te may be the nucleus at the critical point of the $U_{\pi\nu}(5)$-$O_{\pi\nu}(6)$ transition and with feature of $SU^*_{\pi\nu}(3)$ symmetry.

The calculated $\rho^2(E0,0_2^+\rightarrow 0_1^+)\times 10^3$ value also exactly reproduced the observed data. Both the theoretical and experimental properties of $E0$ transition indicate that the 0_2^+ state in ^{124}Te may be interpreted as the lowest state of the first-excited family of intrinsic levels at the critical point of second-order $U_{\pi\nu}(5)$-$O_{\pi\nu}(6)$ transition. Therefore, we conclude that the ^{124}Te is a possible nucleus at the critical point of the second-order phase transition from vibration to unstable rotation, and such a critical point exhibits a slight triaxial rotation. The 0_2^+ state in ^{124}Te can be interpreted as the lowest state of the first-excited family of intrinsic levels in the critical point symmetry. However, it should be mentioned that some of the measured $B(E2)$ and $B(M1)$ values have a large uncertainty and the experimental data of $B(M1,1_1^+\rightarrow 0_2^+)$ is still missing. More theoretical and experimental investigations should focus on these aspects.

We are grateful to Prof. CaiWan Shen, and Dr. XiaoBao Wang of Huzhou University, Prof. YuXin Liu of Peking University, and Prof. GuiLu Long of Tsinghua University for their helpful discussions and good suggestions.

References

1 P. E. Garrett, J. L. Wood, and S. W. Yates, Phys. Scr., **93**: 063001 (2018)
2 L. C. He, Y. Zheng, L. H. Zhu et al, Chin. Phys. C, **41**: 044003 (2017)
3 S. F. Hicks, J. R. Vanhoy, P. G. Burkett, B. R. Champine, S. J. Etzkorn P. E. Garrett, S. W. Yates, and Minfang Yeh, Phys. Rev. C, **95**: 034322 (2017)
4 P. E. Garrett, J. Phys. G: Nucl. Part. Phys., **43**: 084002 (2016)
5 H. Sabria, Z. Jahangirib, and M. A. Mohammadia, Nucl. Phys. A, **946**: 11 (2016)
6 M. Saxena, R. Kumar, A. Jhingan, S. Mandal, A. Stolarz, A. Banerjee, R. K. Bhowmik, S. Dutt, J. Kaur, V. Kumar, M. Modou Mbaye, V. R. Sharma, and H.-J. Wollersheim, Phys. Rev. C, **90**: 024316 (2014)
7 K. Heyde, Rev. Mod. Phys., **83**: 1467 (2011)
8 T. Kibédi, and R. H. Spear, At. Data Nucl. Data tables, **89**: 77 (2005)
9 R. M. Clark, M. Cromaz, M. A. Deleplanque, M. Descovich, R. M. Diamond, P. Fallon, I. Y. Lee, A. O. Macchiavelli, H. Mahmud, E. Rodriguez-Vieitez, F. S. Stephens, and D. Ward, Phys. Rev. C, **69**: 064322 (2004)
10 D. G. Ghiță, G. Căta-Danil, D. Bucurescu, I. Căta-Danil, M. Ivascu, C. Mihai, G. Suliman, L. Stroe, T. Sava, and N. V. Zamfir, Int. J. Mod. Phys. E, **17**: 1453 (2008)
11 E. Guliyev, A. A. Kuliev, P. von Neumann-Cosel, and A. Richter, Phys. Lett. B, **532**: 173 (2002)

12 F. Iachello, Phys. Rev. Lett., **85**: 3580 (2000)
13 F. Iachello, Phys. Rev. Lett., **87**: 052502 (2001)
14 D. Bonatsos, D. Lenis, D. Petrellis, P. A. Terziev, and I. Yigitoglu, Phys. Lett. B, **621**: 102 (2005)
15 Y. Zhang, F. Pan, Y. X. Liu, Y. A. Luo, and J. P. Draayer, Phys. Rev. C, **96**: 034323 (2017)
16 F. Iachello and A. Arima, *The Interacting Boson Model* (Cambridge, England: Cambridge University Press, 1987)
17 M. A. Caprio, and F. Iachello, Ann. Phys., **318**: 454 (2005)
18 P. Cejnar and J. Jolie, Prog. Part. Nucl. Phys., **62**: 210 (2009)
19 P. Cejnar, J. Jolie, and R. F. Casten, Rev. Mod. Phys., **82**: 2155 (2010)
20 T. Naz, G. H. Bhat, S. Jehangir, S. Ahmad, and J. A. Sheikh, Nucl. Phys. A, **979**: 1 (2018)
21 T. Otsuka, Hyperfine interactions, **75**: 23 (1992)
22 Y. Zhang, F. Pan, Y. X. Liu, Y. A. Luo, and J. P. Draayer, Phys. Rev. C, **90**: 064318 (2014)
23 N. Pietralla, P. von Brentano, and A. F. Lisetskiy, Prog. Part. Nucl. Phys., **60**: 225 (2008)
24 D. L. Zhang, S. Q. Yuan, and B. G. Ding, Chin. Phys. C, **39**: 074102 (2015)
25 Y. Zhang, Y. X. Liu, F. Pan, Y. Sun, and J. P. Draayer, Phys. Lett. B, **732**: 55 (2014)
26 A. Giannatiempo, A. Nannini, A. Perego, P. sona, M. J. G. Borge, K. Riisager, O. Tengblad, and ISOLDE Collaboration, Phys. Rev. C, **47**: 521 (1993)
27 D. L. Zhang and C. F. Mu, Chin. Phys. C, **47**: 034101 (2018)
28 J. R. Vanhoy, J. A. Tanyi, K. A. Crandell, T. H. Churchill, S. F. Hicks, M. C. Burns, P. A. Roddy, N. V. Warr, T. B. Brown, and S. R. Lesher, Phys. Rev. C, **69**: 064323 (2004)
29 S. J. Robinson, W. D. Hamilton, and D. M. Snelling, J. Phys. G: Nucl. Part. Phys., **9**: 961 (1983)
30 J. Kern, P. E. Garrett, J. Jolie, and H. Lehmann, Nucl. Phys. A, **593**: 21 (1995)
31 S. Pascu, N. V. Zamfir, Gh. Căta-Danil, and N. Mărginean, Phys. Rev. C, **81**: 054321 (2010)
32 J. Rikovska, N. J. Ston, P. M. Walker, and W. B. Walters, Nucl. Phys. A, **505**: 145 (1989)
33 N. Warr, S. Drissi, P. E. Garrett, J. Jolie, J. Kem, H. Lehmann, S. J. Mannanal, and J. P. Vorlet, Nucl. Phys. A, **636**: 379 (1998)
34 A. Subber, W. D. Hamilton, P. Park, and K. Kumar, J. Phys. G: Nucl. Part. Phys., **13**: 161 (1987)
35 H. Dejbakhsh, D. Latypov, G. Ajupova, and S. Shlomo, Phys. Rev. C, **46**: 2326 (1992)
36 D. L. Zhang and B. G. Ding, Sci. China-Phys. Mech. Astron., **57**: 447 (2014)
37 D. L. Zhang and C. F. Mu, Chin. Phys. Lett., **33**: 102102 (2016)
38 N. Pietralla, T. Mizusaki, P. von Brentano, R. V. Jolos, T. Otsuka, and V. Werner, Phys. Rev. C, **57**: 150 (1998)
39 T. Otsuka and N. Yoshida, Program NPBOS, JAER-M Report, No.85 (1985) (unpublished)
40 T. von Egidy, H.-F. Wirth, I. Tomandl, and J. Honzátko, Phys. Rev. C, **74**: 034319 (2006)
41 K. Nomura, T. Otsuka, N. Shimizu, and L. Guo, Phys. Rev. C, **83**: 041302 (2011)
42 K. Nomura, T. Otsuka, and P. V. Isacker, J. Phys. G: Nucl. Part. Phys., **43**: 024008 (2016)
43 D. L. Zhang and C. F. Mu, Sci. China-Phys. Mech. Astron., **60**: 042011 (2017)
44 K.-H. Kim, A. Gelberg, T. Mizusaki, T. Otsuka, and P. von Brentano, Nucl. Phys. A, **604**: 163 (1996)
45 E. Elhami, J. N. Orce, S. Mukhopadhyay, S. N. Choudry, M. Scheck, M. T. Mcellistrem, and S. W. Yates, Phys. Rev. C, **75**: 011301 (2007)
46 D. L. Zhang and C. F. Mu, Sci. China-Phys. Mech. Astron., **59**: 682012 (2016)
47 J. Rikovska, N. J. Stone, P. M. Walker, and W.B. Walters, Nucl. Phys. A, **505**: 145 (1989)
48 C. Doll, H. Lehmann, H.G. Börner, and T. von Egidy, Nucl. Phys. A, **672**: 3 (2000)
49 S. F. Hicks, J. R. Vanhoy, and S. W. Yates, Phys. Rev. C, **78**: 054320 (2008)
50 G. Mardirosian and N. M. Steward, Z. Phys. A, **315**: 213 (1984)
51 R. F. Casten and N.V. Zamfir, Phys. Rev. Lett., **85**: 3584 (2000)
52 R. F. Casten, D. D. Warner, Rev. Mod. Phys., **60**: 389 (1988)
53 F. Iachello, and N. V. Zamfir, Phys. Rev. Lett., **92**: 212501 (2004)
54 Y. Zhang, Z. F. Hou, and Y. X. Liu, Phys. Rev. C, **76**: 011305 (2007)
55 D. Bonatsos, E. A. McCutchan, R. F. Casten, and R. J. Casperson, Phys. Rev. Lett., **100**: 142501 (2008)
56 J. Stachel, P. Van Isacker, and K. Heyde, Phys. Rev. C, **25**: 650 (1982)
57 P. Van Backer, K. Heyde, J. Jolie, and A. Sevrin, Ann. Phys., **171**: 253 (1986)
58 A. Sevrin, K. Heyde, and J. Jolie, Phys. Rev. C, **36**: 2621 (1987)
59 R. Georgii, T. von Egidy, J. Klora, H. Lindner, U. Mayerhofer, J. Ott, W. Schauer, P. von Neumann-Cosel, A. Richter, C. Schlegel, R. Schulz, V. A. Khitrov, A. M. Sukhovoj, A. V. Vojnov, J. Berzins, V. Bondarenko, P. Prokofjevs, L. J. Simonova, M. Grinberg, and Ch. Stoyanov, Nucl. Phys. A, **592**: 307 (1995)
60 S. F. Hicks, J. C. Boehringer, N. Boukharouba, C. Fransen, S. R. Lesher, J. M. Mueller, J. R. Vanhoy, and S. W. Yates, Phys. Rev. C, **86**: 054308 (2012)
61 D. L. Zhang and C. F. Mu, Sci. China-Phys. Mech. Astron, **61**: 012012 (2018)
62 K. Nomura, R. Rodríguez-Guzmán, and L. M. Robledo, Phys. Rev. C, **95**: 064310 (2017)
63 A. Leviatan and D. Shapira, Phys. Rev. C, **93**: 051302 (2016)
64 J. L. Wood, E. E. Zganjar, C. E. Coster, and K. Heyde, Nucl. Phys. A, **651**: 323 (1999)
65 A. Giannatiempo, A. Nannini, A. Perego, and P. Sona, Phys. Rev. C, **44**: 1844 (1991)
66 O. Möller, N. Warr, J. Jolie, A. Dewald, A. Fitzler, A. Linnemann, K. O. Zell, P. E. Garrett, and S. W. Yates, Phys. Rev. C, **71**: 064324 (2005)
67 C. Qi, Phys. Rev. C, **94**: 034310 (2016)
68 M. Doncel, T. Bäck, C. Qi, D. M. Cullen, D. Hodge, B. Cederwall, M. J. Taylor, M. Procter, M. Giles, K. Auranen, T. Grahn, P. T. Greenlees, U. Jakobsson, R. Julin, S. Juutinen, A. Herzáň, J. Konki, J. Pakarinen, J. Partanen, P. Peura, P. Rahkila, P. Ruotsalainen, M. Sandzelius, J. Sarén, C. Scholey, J. Sorri, S. Stolze, and J. Uusitalo, Phys. Rev. C, **96**: 051304 (2017)